Chemical Engineering Journal 423 (2021) 130141

Contents lists available at ScienceDirect

Chemical Engineering Journal

journal homepage: www.elsevier.com/locate/cej

Partial oxidation of methanol to formaldehyde in an annular reactor

Stine Lervold [a,1], Rune Lødeng [b], Jia Yang [a], Johan Skjelstad [c], Kristin Bingen [d], Hilde J. Venvik [a,*]

[a] Dept. of Chemical Engineering, NTNU - Norwegian University of Science and Technology, NO-7491 Trondheim, Norway
[b] SINTEF Industry, NO-7465 Trondheim, Norway
[c] K.A. Rasmussen AS, NO-2316 Hamar, Norway
[d] Dynea AS, NO-2004 Lillestrøm, Norway

A B S T R A C T

A structured reactor with annular configuration was applied for studying methanol oxidation to formaldehyde over silver. By eliminating gas phase reactions, high formaldehyde selectivity (93–97%) was obtained at low methanol and oxygen conversion under practically isothermal reaction conditions. CH_2O and CO_2 were the only carbon containing products, and both may be claimed as primary products along with H_2. It also proves that CO is formed by homogenous decomposition of CH_2O and should not be considered a main precursor to CO_2, as assumed in several reaction mechanisms. The analysis of H_2/CO_2 ratio as a function of temperature provides an estimate of contributions from dehydrogenation and partial oxidation of methanol, and clearly suggests presence of a dehydrogenation pathway to CH_2O. Extracting kinetic parameters is challenging due to a correlation between activity, oxygen dissolution, and silver restructuring and morphology and its dependence on temperature. Nevertheless, the data indicate 1st order with respect to oxygen. Conditioning by reaction at high temperature followed by a temperature ramp was performed to minimize the impact of a gradually changing Ag catalyst. The resulting Arrhenius analysis implies two distinct regions of activity. The apparent activation energy was estimated to 41 kJ/mol for the high temperature region, a value close to the activation energy for oxygen diffusion in silver at high temperature. The investigation demonstrates benefits of using an annular reactor configuration in bridging lab scale investigations with industrial conditions. Collecting reaction data at low oxygen conversion is enabled, which has not been achievable in conventional lab scale reactors this far.

1. Introduction

The silver catalyzed partial oxidation of methanol to formaldehyde (MTF) is an essential industrial process. Formaldehyde's largest use is in the production of resins for the wood panel industry, but due to its versatile nature as a chemical building-block and its high reactivity, it is applied in the synthesis of various polymers, adhesives and chemical intermediates. Consequently, a wide range of applications such as construction, aviation, automotive, pharmaceuticals and cosmetics are dependent upon formaldehyde [1,2].

Two different process technologies are used in industrial formaldehyde production. The silver-catalyzed process is performed over electrolytically produced silver particles at air lean conditions and 600–700 °C, while the process using mixed metal oxide (iron, molybdenum and/or vanadium) proceeds in excess air and at lower temperature, 250–400 °C. The large-scale silver-catalyzed process accounts for approximately 55% of industrial formaldehyde manufacture. It is operated adiabatically at close to atmospheric pressure by feeding a mixture of methanol vapor, steam and air through a shallow bed of electrolytic silver with a catalyst lifetime of 4 weeks to 12 months [1]. Contact times in the millisecond range over the ~10 mm silver bed are sufficient to ensure complete conversion of oxygen and high methanol conversion. Albeit the fast reactions and hence a reasonable assumption, the role of mass transfer is not clearly stated in the research literature, i.e. there still seems to lack direct evidence for or against the occurrence of diffusion limitations in the industrial reactors [3]. 90–92% selectivity to formaldehyde is achieved with careful selection of CH_3OH/O_2 feed ratio, short residence time, addition of H_2O, and rapid quenching of reaction products. However, 8 to 10% of the methanol feedstock is non-selectively oxidized to carbon dioxide and water/hydrogen, representing production loss and emissions. Economic incentives therefore exist to improve the process selectivity beyond today's state of the art. The product distribution from methanol oxidation over silver may be represented by the reaction equations below (Eqs. 1–9). Traditionally, formaldehyde formation is regarded as a combination of dehydrogenation and partial oxidation of methanol (Eqs. (1) and (2)). $O_{(a)}$ in Eq. (1) represents some form of chemisorbed atomic oxygen on silver, although not necessarily a single species, accounting for the fact that very low conversion is obtained in absence of O_2 in the feed [4–9].

* Corresponding author.
E-mail address: Hilde.j.Venvik@ntnu.no (H.J. Venvik).
[1] Present address: Equinor ASA Trondheim, NO-7053 Ranheim, Norway

https://doi.org/10.1016/j.cej.2021.130141
Received 29 January 2021; Received in revised form 22 April 2021; Accepted 26 April 2021
Available online 4 May 2021

$$CH_3OH_{(g)} \xrightarrow{O_{(a)}} CH_2O_{(g)} + H_{2_{(g)}}, \quad \Delta H = +84\frac{kJ}{mol} \tag{1}$$

$$CH_3OH_{(g)} + \frac{1}{2}O_2 \rightarrow CH_2O_{(g)} + H_2O_{(g)}, \quad \Delta H = -159\frac{kJ}{mol} \tag{2}$$

$$CH_3OH_{(g)} + \frac{3}{2}O_2 \rightarrow CO_{2(g)} + 2H_2O_{(g)}, \quad \Delta H = -676\frac{kJ}{mol} \tag{3}$$

$$CH_3OH_{(g)} \rightarrow CO_{(g)} + 2H_2, \quad \Delta H = +91\frac{kJ}{mol} \tag{4}$$

$$CH_2O_{(g)} + O_2 \rightarrow CO_{2(g)} + H_2O_{(g)}, \quad \Delta H = -519\frac{kJ}{mol} \tag{5}$$

$$CH_2O_{(g)} + \frac{1}{2}O_2 \rightarrow CO_{2(g)} + H_{2(g)}, \quad \Delta H = -271\frac{kJ}{mol} \tag{6}$$

$$CH_2O_{(g)} \rightarrow CO_{(g)} + H_{2(g)}, \quad \Delta H = +12\frac{kJ}{mol} \tag{7}$$

$$H_{2(g)} + \frac{1}{2}O_2 \rightarrow H_2O_{(g)}, \quad \Delta H = -243\frac{kJ}{mol} \tag{8}$$

$$CO_{(g)} + \frac{1}{2}O_2 \rightarrow CO_{2(g)}, \quad \Delta H = -283\frac{kJ}{mol} \tag{9}$$

Silver takes a face centered cubic (fcc) lattice in the metallic state and the dense (1 1 1) planes represent the preferred surface termination in absence of adsorbates [5–7]. It is one of the metals capable of dissolving atomic oxygen, and oxygen solubility and permeability measurements were already performed in the early 1900s [10,11]. Electrolytic silver is known to have a characteristic rough structure resulting from relatively large interconnected crystallites [12–14]. Post reaction, surface restructuring and pinhole formation are evident. The dissolution kinetics as well as the Ag surface mobility are facile above the Tammann temperature (370 °C), and pronounced morphological changes in the Ag catalyst, such as refacetting, sintering, and annealing of grain boundaries and dislocations, are therefore prevalent under MTF reaction conditions [4–7,12–22]. Incorporation and diffusion of atomic surface oxygen in the crystal lattice may hence form a reservoir of oxygen, and do play a role in the structural changes induced.

Understanding the mechanisms, kinetics and active sites for Equation 1–9 is crucial to improve process selectivity towards formaldehyde. However, the actual mechanism of formaldehyde formation is disputed and kinetic data at industrially relevant conditions are limited. Bhattacharyya et al.[23] investigated the kinetics of methanol oxidation over metallic silver in the temperature range 264–290 °C at low conversion. A tentative mechanism, applying a “steady-state-adsorption (SSA)” model, proposed the formation of formaldehyde from oxidation of methanol by adsorbed oxygen, whereas CO_2 was formed by complete oxidation of methanol with adsorbed oxygen or oxidation of formaldehyde with gaseous/adsorbed oxygen. The reaction order was suggested to be dependent on feed composition and they estimated an overall reaction order of 0.5 to oxygen and nearly zero order to methanol at low oxygen concentration. Robb and Harriot [24] applied a diluted porous alumina supported silver catalyst at an intermediate temperature of 420 °C. They observed an almost zero-order dependence on oxygen (except at very low pressures) and slightly less than first order to methanol. These studies were performed in more conventional laboratory packed beds, where the high conversion of oxygen prohibited the extraction of kinetic data in the industrially relevant temperature range. It is difficult to balance gas flow, available catalyst surface and reactor design to avoid high conversion of oxygen at elevated temperature without introducing thermal gradients, feed bypass or mass transfer limitations when it comes to fast and exothermic oxidation reactions. With respect to methanol oxidation, ensuring survival of the formaldehyde product is also critical. O_2 will consume formaldehyde through radical gas phase reactions at prolonged residence time with temperatures exceeding ~450 °C[3–6,9,25–28] and formaldehyde alone decomposes to CO and H_2 in excess of 350 °C [2]. Moreover, varying the reactant composition will affect the mechanistic scheme and the interaction between Ag and oxygen, and thereby the product formation.

Wachs and Madix [25] used UHV-TPRS to study the adsorption and oxidation of CH_3OH on a Ag(1 1 0) crystal surface. They found that CH_3OH adsorbed reversibly on clean Ag(1 1 0) surfaces at low temperature (-75–25 °C). In the presence of pre-adsorbed atomic oxygen, however, CH_3OH dissociated to form H_2O and surface methoxy species. The amount of chemisorbed methanol increased as a function of oxygen exposure, showing that adsorbed atomic oxygen must be present to promote formation of methoxy and the consecutive decomposition to formaldehyde or further oxidation to carbon dioxide from a formate intermediate. In the simplified reaction mechanism presented, chemisorbed atomic oxygen (O_α) was claimed to be the only active oxygen species in the mechanism and a direct reaction pathway from methanol to carbon dioxide was not included. Similar schemes were also reported for methanol oxidation on Ag(1 1 1) and polycrystalline silver surfaces under UHV conditions [29,30]. Andreasen et al. [26,31] used this model as a basis for developing a microkinetic model for oxidation of methanol to formaldehyde and oxidation of formaldehyde to carbon dioxide . Only one type of atomic oxygen was included in the elementary reaction system, i.e. O_α, claiming that this species could explain industrial formaldehyde synthesis at steady-state conditions.

Three distinct atomic oxygen species have been proposed as resulting from the adsorption on, and dissolution of O_2 in, Ag at temperatures and pressures representative of industrial formaldehyde manufacture, denoted O_α, O_β and O_γ [3–8,15–18,20–22,25,28–30,32–37]. These species' features vary in location, Ag-O bonding and thermal stability. Molecular oxygen dissociates on the silver surface and forms the weakly chemisorbed surface O_α species. At high surface coverage, bulk-dissolved, silver sub-oxide O_β forms from diffusion of O_α into the Ag lattice. The strongly chemisorbed oxygen species O_γ is discussed to originate from O_β when the latter segregates from bulk to the surface at high temperature and exist predominantly in the uppermost layers of the silver catalyst. The population of these species strongly depends on pretreatment, temperature and exposure, and their relevance to various pathways are still under debate. A significant amount of experimental results supports the low temperature dominance (~325 °C) of O_α and its participation both in forming formaldehyde from methanol and in the non-selective oxidation of methanol and formaldehyde to CO_2 (Eqs. (3), (5) and (6)) [4–7,16,18,32,38]. Qian et al. [9] also found evidence of O_α to benefit the formation of HCOOH. Since several investigations claim the existence or importance of one oxygen species only, i.e. O_α , the role of O_γ in the methanol oxidation is the most debated. Schubert et al. [8,39], Nagy et al. [5–7], Qian et al. [9] and Schlunke et al. [40] identified O_γ as the active site for dehydrogenation of methanol (Eq. (1)), with the continuous supply from O_β being significant for the catalytic properties. Beuhler et al.[38], van Veen et al. [32] and Waterhouse et al. [4] agree that the transformation of O_β to O_γ is important but implied a highly selective oxidative pathway to formaldehyde and water (Eq. (2)) with O_γ, rather than the direct dehydrogenation route. Bao et al. [16] illustrated how the presence of water could change the oxygen dynamics on the silver surface at high temperatures. H_2O was found to promote the formation of surface O_γ on the silver surface, which could be relevant for selective oxidation of methanol to formaldehyde.

To overcome the challenges associated with investigating partial oxidation (POX) processes with fast kinetics and strong temperature effects, short contact time reactors such as annular and catalytic wall reactors have successfully been applied to gain kinetic and mechanistic insight [27,41–48] . The annular reactor concept offers a controlled system with laminar flow and negligible backmixing, close to isothermal conditions, negligible mass transfer limitations and quenching/suppression of reactions in the gas phase [43,44,48–52]. In addition, annular reactors can help bridge lab-scale investigations with industrial operation by enabling

kinetic investigations at high space velocity and high reaction temperature. Compared to the more traditional laboratory packed bed reactors, large pressure gradients caused by high flow rates, and non-uniform temperature profiles can be avoided. Most important, low conversion to obtain insight into the primary characteristics of the reaction can be achieved without compromising on temperature and formaldehyde selectivity. Cao et al. [27] investigated oxidative dehydrogenation of methanol in microstructured reactors, and the results demonstrated the benefits of using narrow reaction channels in the study of highly exothermic reactions. Their results indicated that the reaction was 0.5 order with respect to methanol, somewhat agreeing with Bhattacharyya et al.[23], Robb and Harriot [24] and Lefferts et al. [3], who all obtained less than first order dependency. Nevertheless, most of Cao et al. [27] studies were performed at 510 °C, still some way from industrial conditions and with no water feed present. Lefferts et al. [35] showed how water affected the selectivity of the MTF reaction, reducing the CO_2 production. Qian et al. [9] also presented the benefit of the water ballast process over methanol ballast with respect to higher conversion of methanol and selectivity to formaldehyde.

In this paper we present results from a first annular reactor experimental series of the catalytic partial oxidation of methanol to formaldehyde over pure silver in presence of water. A range of temperatures, oxygen concentrations and residence times were investigated to arrive at some direct conclusions on what may be regarded as primary and secondary products. The potential of the annular reactor concept for studying reaction kinetics is demonstrated and some kinetic parameters can be estimated despite interference with the abovementioned morphology changes resulting from Ag restructuring and oxygen dissolution.

2. Materials and methods

2.1. Catalyst and experimental setup

A structured reactor with annular configuration was adapted to partial oxidation of methanol over an Ag surface and the reactor assembly is shown in Fig. 1. High purity, polycrystalline silver rods (99.95%; Goodfellow) are modified to Ag catalyst tubes (ID/OD of 4/10 mm), into which an internal quartz duct is inserted with a tight fit and a wider section below the tube of similar diameter to keep it in place. This assembly is then placed internally to the quartz reactor (length" 420 mm, ID"11 mm and OD"14 mm). A quartz piece of similar radial dimensions as the catalyst and length extending towards the inlet is also placed on top (see Fig. 1). This geometry is intended to minimize the dead volume and changes in the flow pattern along the whole reactor length. The gas stream flows between the two tubes constituting an annulus with hydraulic diameter of ~ 1 mm. A laminar regime and high linear gas velocity can be achieved with practically no pressure drop, and negligible contributions from the inside and end surfaces of the Ag catalyst tube. A thermocouple sliding inside the quartz duct was used to measure the axial temperature profile. A temperature programmed (Eurotherm) two-zone annular furnace with preheat and reaction sections was used to heat the reactor. The experimental setup has stainless-steel pipelines equipped with mass flow controllers (Bronkhorst) for synthetic air, nitrogen and helium. A pressurized stainless-steel container is used for methanol/steam feed, which is regulated by a liquid flow controller with an integrated evaporator (Bronkhorst).

A gas chromatograph (GC) is used for analysis of feed and product composition (Agilent Technologies 7890A) and all pipelines following the evaporator are heat-traced at a temperature of 120–140 °C. The GC contains four columns; two Hayesep A columns are installed before its two main columns, a PLOT molsieve (Ar carrier gas) to separate light gases (H_2, O_2, CH_4, CO and N_2) and a WCOT CP-sil column (He carrier gas) to separate compounds based on boiling point (CH_4, CO_2, CH_3OH, CH_2O, HCOOH and H_2O). Both columns are connected to thermal conductivity detectors (TCD). Nitrogen was used as internal standard and relative response factors were estimated on the basis of calibrated gas and liquid ($CH_2O/CH_3OH/H_2O$ = 37/8/55 wt%) mixtures. Due to the challenges of H_2O quantification in this system, only the carbon balances were closed within 5% deviation under all conditions. The conversion, X, is defined as converted reactant based on the molar flow of reactant (CH_3OH, O_2) converted, and expressed as a percentage:

$$X_{CH_3OH/O_2}\ [\%] = \frac{F_{CH_3OH/O_2,\ in} - F_{CH_3OH/O_2,\ out}}{F_{CH_3OH/O_2,\ in}}$$

Selectivity, S [%], based on products is used for CH_2O and CO_2 as indicated below, since only two carbon products are present and C-balances closed:

$$S_{CH_2O/CO_2}\ [\%] = \frac{F_{CH_2O/CO_2}}{F_{CH_2O} + F_{CO_2}}$$

A mass balance analysis for H and O, comparing feed analysis and products formed, allowed the H_2O selectivity to be calculated. The presented H_2 and H_2O selectivities are based on the H mass balance as the molar product flow per molar flow of methanol consumed:

$$S_{H_2O/H_2}\ [\%] = \frac{F_{H_2O/H_2,\ out}}{F_{CH_3OH,\ in} - F_{CH_3OH,\ out}}$$

2.2. Experimental protocol

Several preliminary experiments for partial oxidation of methanol over Ag in the annular (and a fixed bed [12]) reactor were conducted to determine reference operating conditions, confirm reproducibility and absence of homogenous gas phase contributions. A high linear gas velocity and limited conversion could be realized for 20 mm long catalyst tube (~13 g of Ag), a total flow rate of 250 Nml/min (volume gas at STP; 0 °C, 101.3 kPa), which corresponds to a linear gas velocity of 0.26 m (STP)/s. A standard feed composition of methanol and water in air and nitrogen with $CH_3OH/H_2O/O_2/N_2$ = 8/11/3/78 molar ratio was applied. This gives a CH_3OH/O_2 ratio of 2.6 and H_2O partial pressure close to typical industrial conditions. Experiments were performed at varying furnace temperatures from 540 to 600 °C at atmospheric pressure to obtain an industrially relevant product distribution in the kinetically controlled regime.

Herein, we report 4-day MTF synthesis experiments at constant temperature in the range 540–600 °C using a fresh separate silver tube for each temperature setpoint (every 20 °C). During those 4 days on stream the effects of varying residence time (50–130 ms, 150–350 Nml/min, 0.1–0.4 m/s at STP) and oxygen partial pressure (1.5, 3 and 6 mol%) were investigated while maintaining all other parameters constant. After the 4-day run, each silver tube was characterized through scanning electron microscopy (Hitachi S-3400 N, 15 kV) to analyze morphological changes.

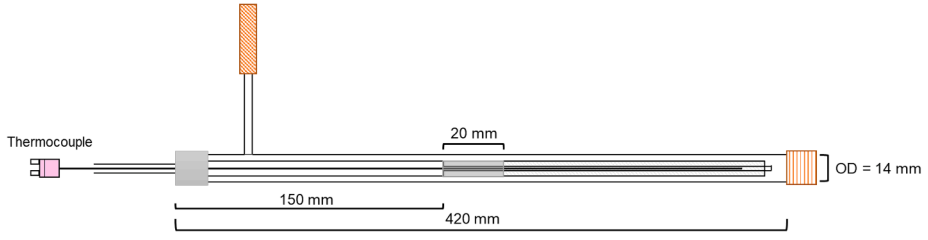

Fig. 1. Schematic of the annular reactor (L:420 mm, ID:11 mm and OD:14 mm).

In addition, because of the changes occurring in the catalyst over 4 days, longer (~8 days) runs with only reference conditions at furnace setpoint 600 °C were performed before stepwise cooling (every 20 °C /2h) to 500 °C. This enabled collecting kinetic data more representative of a morphological steady-state of the catalyst.

3. Results and discussion

3.1. Effect of temperature on conversion, selectivity, and bed temperature

Results from a series of experiments at constant furnace temperature setpoint from 540 to 600 °C, each employing a fresh 20 mm Ag catalyst tube and maintained for 4 days on stream, are first presented. The reaction was carried out as described in Section 2.2, switching between the reference reactant composition and flow rate, and intervals of varying only flow or only the oxygen partial pressure. Fig. 2a-e show the methanol and oxygen conversion, carbon selectivity to formaldehyde and carbon dioxide, and hydrogen to carbon dioxide molar ratio as function of time on stream (total) under reference conditions only. The duct temperature measured inside the quarts pocket inserted into the Ag tube is also shown (Fig. 2f). This series illustrates some main features of the reaction and the annular reactor concept.

The conversion of methanol (Fig. 2a) and oxygen (Fig. 2b) could both be maintained well below 100% throughout the experiments, while the formaldehyde selectivity is 93–97% (Fig. 2c). As explained in the introduction, incomplete oxygen conversion is difficult to realize in fixed bed experiments under temperatures and reactant compositions (CH_3OH/O_2) relevant to industrial operation. Fig. 2 hence demonstrates that our experimental approach allowed establishing conditions where the homogenous reactions are of no significance; essentially the annular geometry in conjunction with two-zone heating and experimental protocol. Cao et al. [27] obtained a similar result by applying a silicon-glass microchannel reactor coated with silver. They conducted experiments with oxygen concentrations throughout and beyond the explosive regime usually omitted in experiments as well as in industrial operation. Qian et al. [9] were also able to perform fixed bed experiments with varying oxygen conversion (30–100%) by extensive dilution of the silver and non-isothermal operation of the reactor. The formaldehyde yields reported at 30% and 80% oxygen conversion correspond to 8% and 87% selectivity, respectively, due to temperature dependent formation of formic acid and CO_2. The temperature dependent trends in CH_3OH and O_2 conversion are otherwise as expected under kinetic control, except for the 540 °C setpoint temperature that will be further discussed below. This is in agreement with Waterhouse et al. [4] and Cao et al. [27] with respect to methanol conversion. Qian et al. [9], however, reported the conversion of methanol as almost constant in the range 525–625 °C.

No CO or formic acid can be detected in the product mixture pertaining to Fig. 2. The only carbon products are formaldehyde and carbon

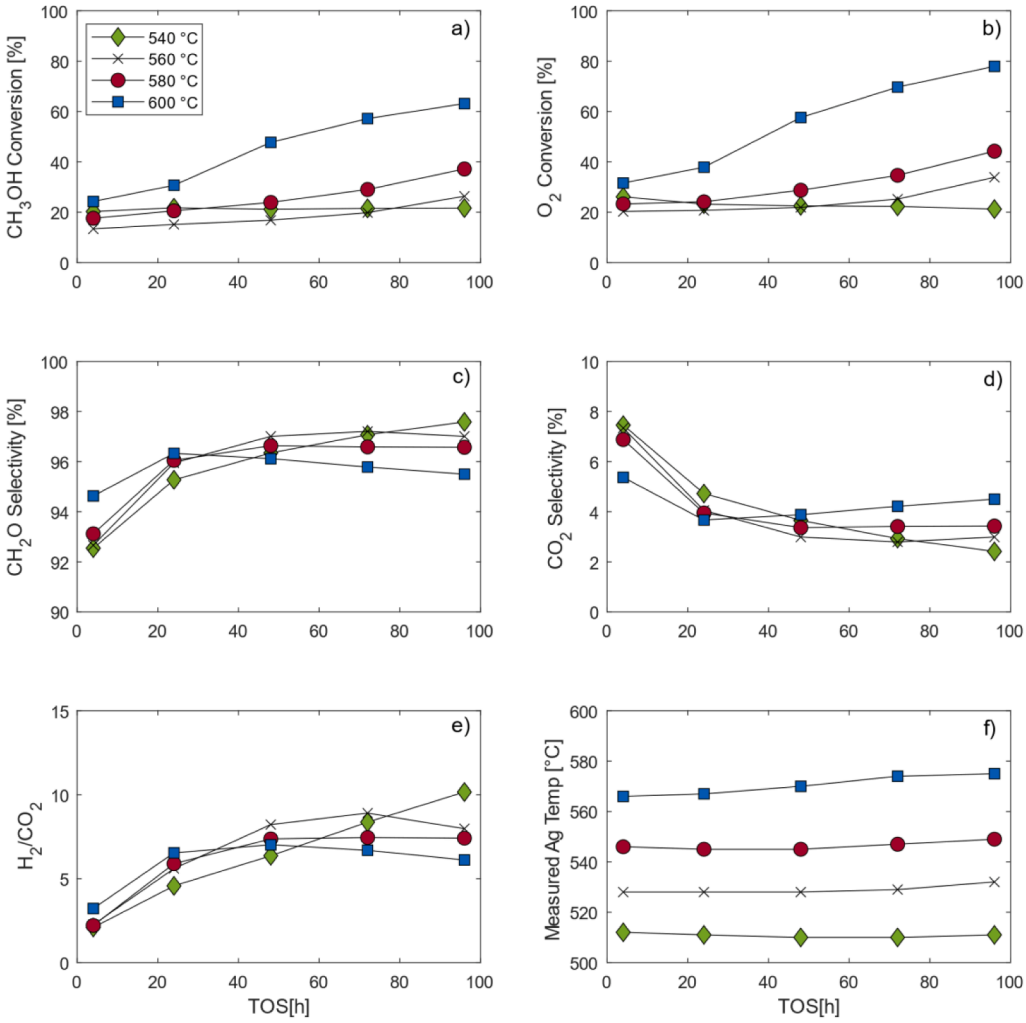

Fig. 2. Reactant consumption, product formation and catalyst temperature at standard reaction composition as a function of time on steam for different furnace setpoint temperatures in the range 540–600 °C. a) and b) CH_3OH and O_2 conversion, c) and d) C-selectivity to CH_2O and CO_2, e) H_2/CO_2 molar ratio f) measured duct temperature within the Ag tube. Molar feed composition $CH_3OH/H_2O/O_2/N_2$ = 8/11/3/78, total flow rate 250 Nml/min, Ag catalyst tube length 20 mm.

dioxide, their selectivities mirroring each other in Fig. 2c-d. Furthermore, experiments not shown here, with the annular reactor or with Ag particle beds composed of commercial catalyst and mostly under complete oxygen conversion, occasionally yield CO. The extent of CO formation consistently correlates with high temperature (>630 °C), longer residence time, or increased dead volume, the latter due to e.g. irregularities (e.g. misaligned Ag tube) in the annulus/bed reactor geometry. This implies that CO is not a primary product, but mainly formed via decomposition of CH_2O to CO and H_2 in the gas phase. It also strengthens the notion that the applied annular reactor concept can suppress homogenous contributions and testifies to the importance of avoiding these to obtain mechanistic insight. The absence of gas phase chemistry also (partly or fully) explains the exceptionally high CH_2O selectivity (93–97%) obtained. It is not straightforward to compare to literature values, but to the extent of our knowledge most studies report selectivities of less than 90% [3–6,9,28,39] while the abovementioned report using a microchannel reactor obtained 93% [27].

Fig. 2f shows the measured quartz pocket temperature as function of time on stream for each furnace setpoint temperature. A correlation between increased conversion and increased bed temperature is apparent, which means that the system is sensitive to the heat produced by the reaction itself. It should be noted that the measured temperature is ~ 30 °C lower than the furnace setpoint, which regulates the power of the heating element against a thermocouple placed close to the element itself. This means that there is a radial gradient between the heating element and the silver tube, as well as between the silver tube and the quartz pocket. Although the largest gradient applies to the former, the actual Ag temperature is always slightly higher than the measured duct temperature. The duct measurements also indicate small temperature gradients (±5 °C) along the silver tube but are of course affected by positioning of the thermocouple. Estimates made by modeling (Comsol Multiphysics) of the reactor geometry, taking into account the high thermal conductivity of Ag as well as the heat supplied and generated, suggest that the actual temperature of the silver tube is practically constant. With respect to the annular reactor concept, it may be conjectured that isothermal conditions are obtained across the catalyst for a given setpoint temperature, but that the temperature measurement and regulation needs to be improved - without affecting the experiment in other ways - to further increase the precision.

From Fig. 2a-e it is clear that the catalytic Ag tubes have not reached a steady-state activity level during the four days on stream, with both the methanol and oxygen conversions continuously increasing and the selectivities slightly changing. The increase in conversion most likely reflects a progressing and temperature dependent restructuring of the Ag surface that is strongly impacted by oxygen dissolution. The diffusivity of oxygen in silver increases with temperature [53,54], likewise the mobility of silver surface atoms. Consequently, the catalyst restructuring occurs on a shorter time scale at higher temperature. The effects become very distinct in the present study due to the low conversions, the absence of gas phase reactions and the application of a bulk silver tube. In industrial formaldehyde manufacture at 650–680 °C the effects of morphological change can be less visible. But it is not possible to directly extract kinetic parameters from this temperature series albeit low conversions, and the initial data points represent a catalyst far from its conditioned (steady-)state.

The selectivity to formaldehyde initially increases with time on stream (Fig. 2c). This process is faster with higher temperature and seems to go through a maximum before a slight decrease proceeds. The time at which the maximum is reached is also temperature dependent, with the 540 °C setpoint displaying $S(CH_2O) > 97\%$ and not being passed its maximum after 90 h. The CO_2 selectivity is the exact opposite, and this suggests that sites critical to formation of formaldehyde are to some extent created initially, while the formation of CO_2 is promoted by unconditioned metallic silver at lower temperature. The latter is in agreement with Nagy et al. [5,6], who found that no morphological change of the catalyst is necessary for Ag to be active. The main reactions proceeding in the initial state were between weakly adsorbed atomic oxygen (O_α) and methanol, with CO_2 being favored at 300 °C and below. They, as well as Waterhouse et al. [13], also assessed the changes occurring upon running a fresh silver catalyst through several reaction temperature cycles. Initially, there were prominent and varying hysteresis effects in the conversion and formaldehyde selectivity. Only after several runs with the same silver catalyst, they obtained reproducible behavior, overall enhanced conversion and CH_2O selectivity, and absence of hysteresis. Our own results from sub-reaction experiments over Ag particle beds showed that the CO oxidation activity and the measured catalyst temperature (670–630 °C) significantly reduced during time on stream alongside an otherwise similar restructuring as under methanol oxidation [12].

The small decrease in formaldehyde selectivity seen after the maximum in Fig. 2 indicates that an equilibrated state of the Ag is still under development for all the temperatures, but that the continued restructuring is not associated with enhancing the formaldehyde selectivity towards 100%. What needs to be established is the extent to which the selectivity is unequivocally affected by conversion, as may be inferred by Fig. 2c. Preliminary experiments at high temperature (not shown) demonstrated, however, that at least 85% selectivity can be sustained at complete conversion of oxygen, but our annular reactor design was not completely optimized to suppress the gas phase chemistry at this stage. The dynamic relationship between O_α and O_γ may take some time to develop and could also be reflected in the product distribution. As activity increases with further restructuring, the formation of O_γ, said to be the selective route to formaldehyde, may not be able to follow by the same rate and a small increase in CO_2 through enhanced presence of O_α could occur.

The H_2/CO_2 molar (Fig. 2e) ratio also reaches a maximum before slowly decreasing for the analyses performed at 560–600 °C. As for the CH_2O selectivity, this proceeds faster at higher temperature, so that the ratio is still increasing at furnace setpoint 540 °C after 4 days on stream. The change in H_2/CO_2 ratio may indicate which reaction (Eq. (1) vs Eq. (2)) that prevails. It was not possible to independently quantify H_2O formation with the equipment applied here but the fact that hydrogen is produced in larger amounts than CO_2, with no CO detected, suggests the presence of a dehydrogenation mechanism. A consecutive mechanism that initially yields CH_2O and H_2O according to Eq. (2) and thereafter formation of CO_2 in 1:1 stoichiometry with H_2 from CH_2O (Eq.6) should give no change in the H_2/CO_2 ratio with varying CO_2 formation. Since the formaldehyde selectivity and the H_2/CO_2 ratio follow the same pattern with respect to temperature and TOS and thermodynamics dictate that endothermic reactions will dominate at higher temperature, it seems likely that a dehydrogenation pathway is the underlying mechanism behind these trends.

3.2. Residence time effects

The effect of residence time was examined in the temperature range 540–600 °C by varying the total flow and keeping the reactant composition constant. The residence time is defined as the ratio of void volume along the catalyst tube to gas volumetric flow rate (at STP). Fig. 3 shows the effect of residence time on conversion and product selectivities for the highest furnace setpoint temperature (600 °C, 567 °C measured duct temperature). Both the methanol and oxygen conversions increase for all temperatures, as expected, while little or no change in the product distribution can be observed in the range of flow rate investigated. This was also the case for the lower temperatures (not shown), only minor variations around 95–96% in the formaldehyde selectivity were obtained at setpoint 540 °C. Notably, neither the measured duct temperature changed with residence time except for the 540 °C case, where a slight increase was detected (~2 °C). The practically constant carbon product distribution across a varying, but low, residence time regime and 29–41% methanol conversion suggests that CH_2O and CO_2 are primary products of partial oxidation of methanol over Ag. Correspondingly, the same can be said for hydrogen and possibly also water based on the H-

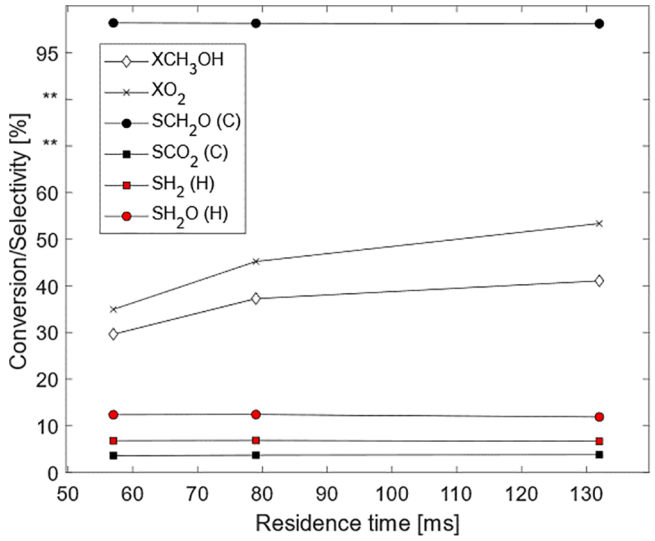

Fig. 3. Conversion (CH_3OH and O_2) and product selectivities (CH_2O, CO_2, H_2 and H_2O) at standard reactant composition as a function of residence time (total flow rate 150, 250 and 350 Nml/min) for the highest furnace setpoint temperature (600 °C, corresponding to 567 °C measured duct temperature). Molar feed composition $CH_3OH/H_2O/O_2/N_2$ = 8/11/3/78, Ag catalyst tube length 20 mm.

balance. Lefferts et al. [3] found no significant change in conversion (~65%) nor selectivity upon increasing the space and linear gas velocity, only an effect on CO formation increasing with decreasing flow rate was apparent. Qian et al. [9] reported a significant decrease in formaldehyde yield with increasing residence time at ~ 550 °C, and attributed this to decomposition of formaldehyde to H_2 and CO in the gas phase at high temperature. No CO was detected for the residence time variations discussed here, but their interpretation fits well with our conjectures in Section 3.1 above. Furthermore, due to the lack of CO, the hydrogen formed can be assumed to be a primary product on the same level as CH_2O and CO_2.

3.3. Oxygen partial pressure

The effect of oxygen partial pressure on the MTF reaction was examined by varying the concentration of oxygen (CH_3OH/O_2 = 1.3–5.3), balancing with nitrogen to keep the total volumetric flow and the methanol and water feed concentration constant. Fig. 4 shows the effect of oxygen on conversion and selectivity as function of – this time – the measured duct temperature. The correlation between measured duct temperature and setpoint temperature for the different concentrations is also shown (Fig. 4h). The former, and hence the reaction temperature, significantly increased with oxygen concentration, which clearly demonstrates why we in this case should consider the duct temperature upon comparing the data points. Due to the placement of the thermocouple regulating the furnace temperature, it proved challenging to adjust the setpoint to ensure constant duct temperature at each oxygen concentration.

Similar to most previous studies [3,4,18,27,28,40], the methanol conversion increases with increasing oxygen concentration (Fig. 4a). Robb and Harriot [24], however, reported the methanol conversion as independent of the oxygen concentration above ca. 1%. But this study was conducted at low temperature (420 °C) and applied a supported silver catalyst, and it cannot be excluded that it is related to support or other effects. The conversion of oxygen is not enhanced accordingly (Fig. 4b), but the molar rate of oxygen consumption roughly doubles with a doubling in the partial pressure for a given temperature. Estimations of reaction order proved challenging as the temperature slightly changed with partial pressure. Moreover, we suspect that the degree of restructuring (e.g. active surface area) and the distribution sites (O_α vs O_γ) are both affected. Nevertheless, the results indicate that the reaction is close to 1st order with respect to oxygen.

The effect on product selectivity is comparable to what has been previously observed [3,4,9,27,40]. The formaldehyde and carbon dioxide selectivities decrease and increase, respectively, with increasing oxygen concentration (Fig. 4c and d) and most pronounced at high temperature. Coupled with the conversion and catalyst temperature profiles, it implies that an increased oxygen partial pressure promotes the total oxidation of methanol albeit oxygen's role in creating sites critical to the formation of formaldehyde through formation of O_γ. Previous studies showing similar results were performed in conventional fixed bed reactors. Cao et al. [27] examined the effect of oxygen in both a quartz tube reactor and a microstructured reactor, the latter offering the possibility of carrying out experiments with oxygen concentrations varying from 3 to 91.4% (CH_3OH/O_2: 2.9–0.1). Results from both reactor setups, notably in absence of water, display similar trends as presented in Fig. 4 at comparable oxygen concentrations. However, the formaldehyde selectivity and methanol conversion changed relatively little when increasing the oxygen concentration beyond 12.5%. The former maintained higher than 90%, and they proposed that an increase in the formation of water with increased O_2 could promote the formation of formaldehyde. Moreover, assuming CO_2 to be formed from reactions of adsorbed formaldehyde, the concentration of surface atomic oxygen species leading to CO_2 could be unaffected by the gas phase oxygen concentration increase beyond a saturation point. Thus, at high oxygen concentrations the reaction order may be close to zero with respect to oxygen.

The hydrogen selectivity and H_2/CO_2 ratio (Fig. 4e and g) change little with temperature, but the effect of oxygen concentration is prominent. CO_2 formation increases and the hydrogen selectivity significantly decreases with increased oxygen concentration, with the estimated (H-based) H_2O selectivity correspondingly increasing (Fig. 4f). A joint increase in CO_2 and H_2O selectivity can be explained by oxidation of methanol (Eq. (3)) and/or formaldehyde (Eq. (5)). Madix and co-workers attributed increased CO_2 formation in the presence of excess surface oxygen to Eq. (6) [25,55]. Here, the molar rate of hydrogen produced is approximately constant for the three oxygen concentrations, except for a small increase at the highest temperature and Eq. (6) cannot alone account for the formation of CO_2. Moreover, silver is active towards hydrogen oxidation [12]. Thus, hydrogen seems to be a primary product that to a large extent survives due to kinetic limitations under methanol oxidation conditions and excess/unconverted oxygen. The increase in methanol conversion coupled with the trend in selectivity could be an indication of methanol being directly combusted to CO_2 and H_2O to a larger extent at increasing temperature and oxygen concentration. This is in agreement with Waterhouse et al. [4] and Lefferts et al. [3,21] suggesting an increase in concentration of weakly adsorbed atomic oxygen (O_α) at decreased CH_3OH/O_2 ratios, often identified as responsible for the non-selective oxidation of CH_3OH and CH_2O. In fact, the constant amount of hydrogen produced could suggest that the pathway trough O_α is promoted by increased oxygen partial pressure, while the pathway through O_γ could be responsible for the dehydrogenation reaction (Eq.1) and independent of the oxygen concentration.

For the case of 1,5 and 3 mol% O_2, the molar rates of oxygen consumed in conjunction with hydrogen formed again imply that a dehydrogenation mechanism must be present. The molar rate of oxygen consumption is not sufficient to account for the formaldehyde and carbon dioxide formation and H_2/CO_2 is>1. For the highest oxygen concentration at 6 mol% of O_2, the need for a dehydrogenation pathway becomes less apparent.

3.4. Reaction-induced changes in the silver catalyst morphology

SEM analyses were applied to obtain an indication of how the changes in annular catalyst performance with time on stream were related to the extent of structural modification. Fig. 5a-b shows SEM images of as-received annular silver and annular silver (30 mm length)

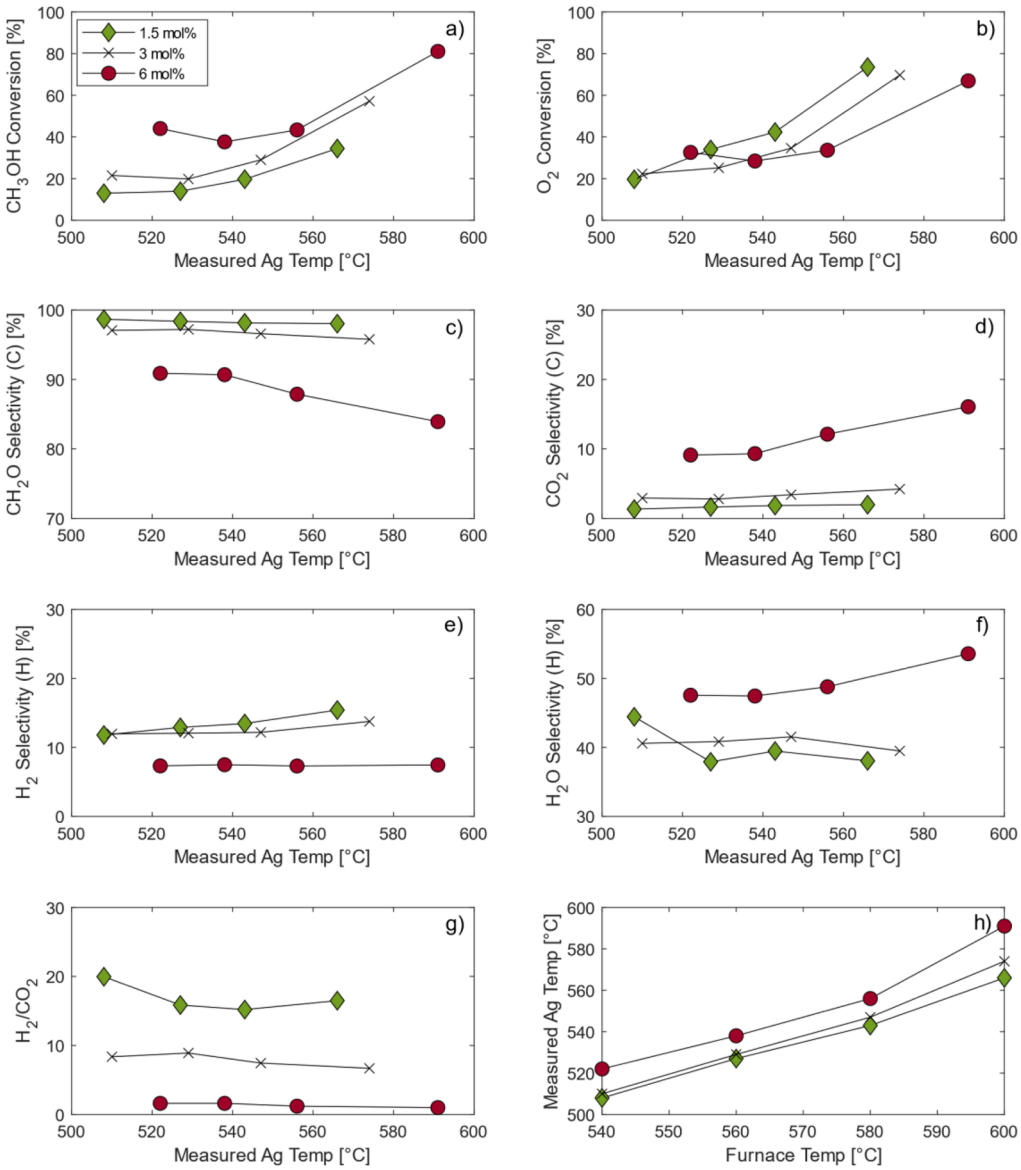

Fig. 4. Effect of oxygen partial pressure (by concentration variation) on reactant consumption and product formation as a function of measured Ag duct temperature: a) and b) CH_3OH and O_2 conversion, c) and d) C-selectivity to CH_2O and CO_2, e) and f) H-Selectivity to H_2 and H_2O, g) H_2/CO_2 molar ratio, h) measured Ag temperature as function furnace setpoint. Reaction conditions: furnace setpoint 540–600 °C, molar feed composition O_2 = 1.5–6 with CH_3OH/H_2O = 8/11 and N_2 as balance, total flow rate 250 Nml/min, Ag catalyst tube length 20 mm.

used for a 15-day long MTF experiment with the standard reactant composition and reaction temperatures in the range 570–655 °C. The unused silver tube (Fig. 5a) shows a relatively flat surface but with marks and slight corrugations resulting from the mechanical machining applied in its preparation. The surface is different from that of electrolytic silver catalyst particles [12], but both materials are characterized by high purity and fcc structure. While the catalyst appearances differ in their fresh state, the morphology presented in Fig. 5b bears strong resemblance to industrially applied silver catalyst as presented in our previous work as well as by others [12–14,19,20,56–58]. The annular catalyst subjected to MTF reaction conditions for 15 days appears more corrugated and a significant number of pinholes have formed. The surface is also refacetted, and close examination often reveals a terraced structure surrounding the pinholes [12,13,18,32]. Pinholes are commonly described as a result of sub-surface oxygen/hydrogen/hydroxyl interactions, resulting in stress induced by the hydrostatic pressure being released to create holes. We recently [12] established pinholes as present in all silver catalyst samples exposed to oxygen at 650 °C, indicating that presence of hydrogen is not prerequisite. Waterhouse et al. [13] compared two silver catalysts from different commercial suppliers and showed that the catalysts differed considerably in their initial surface morphology and specific surface area, which in turn impacted their initial catalytic properties. However, the two catalysts eventually became indistinguishable in their morphology and performance.

The SEM micrographs of Fig. 5c-f indicate that the annular silver gradually develops a surface morphology comparable to that observed on conventional (electrolytic) Ag particle catalysts post reaction. Each sample represents a different, practically constant, reaction temperature, but otherwise approximately equal exposure in terms of duration and parameter variations (residence time and oxygen concentration). The extent of morphological change, and hence the rate of the restructuring phenomena involved, is clearly temperature dependent. For the furnace temperature setpoint of 540 °C (Fig. 5c) a substantial number of pinholes are present, and the surface appears somewhat smoothened yet more corrugated than in Fig. 5a. The same characteristics are present for higher temperature (Fig. 5d-f), but an increasing amount of protrusions is found. Steacie et al. [11] investigated the solubility of oxygen in silver and found that it increases above 400 °C. They furthermore addressed the concept of how molten silver absorb oxygen from air and then "spits" upon solidification. The reaction temperatures applied in the present work were never close to the melting point (962 °C), but due to the

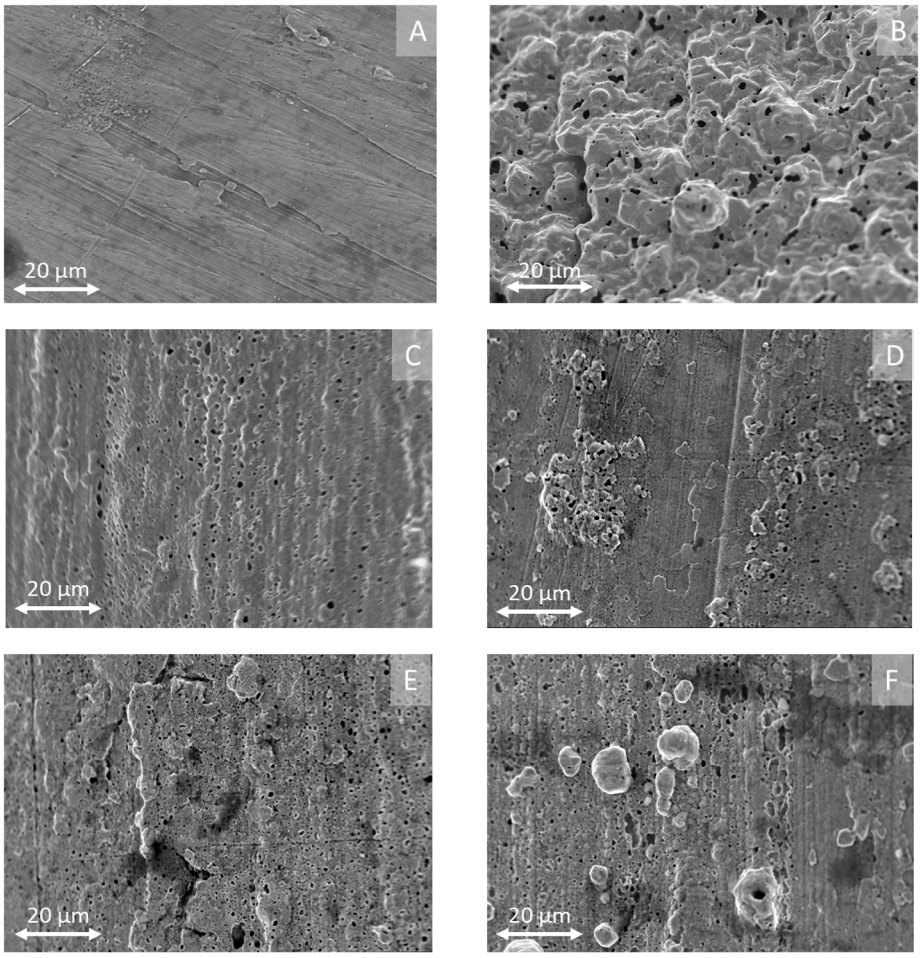

Fig. 5. SEM micrographs of the outer silver surface pre and post MTF reaction for 6 annular Ag samples: a) as-received, unused silver, b) after 15-day experiment at reaction temperatures in the range 570–690 °C and varying reactant composition and flow, c)-f) after 4 days on stream under varying reactant composition and flow at constant furnace setpoint of c) 540 °C, d) 560 °C, e) 580 °C, and f) 600 °C. Ag catalyst tube length a) NA, b) 30 mm, c)-f) 20 mm.

mobility of silver above Tammann temperature, it seems likely that oxygen dissolution has caused "silver spitting" in addition to pinhole formation. Due to the more corrugated structure of the commercially applied silver particle catalyst, it is difficult to determine whether "spitting" is present also in that system. However, Millar et al. [14,56] observed a similar phenomenon, with extensive changes initiated in the appearance of the polycrystalline silver surface during methanol oxidation at 570 °C. The entire surface was described as covered by small protrusions, referred to as "nodules", which resemble those visible in Fig. 5. The "nodules" were reported to increase in size with progressed reaction and by increasing the temperature, they found violent eruptions to produce micrometer sized holes over the entire surface and it was noted that these originated at "nodule" sites. A similar process may have occurred in our experiment performed at 600 °C (Fig. 5f). It should be noted that dissolution of oxygen (and hydrogen/hydroxyl) causes gradients and lattice expansion in the silver that induce stress in the material, and that the extent of spitting and other restructuring likely are consequences of strain. These may be significantly different between the (somewhat loosely) packed electrolytic silver particles subject to most investigations, and the bulk silver tube applied here. While the former may to some extent expand in all directions, the latter is more constrained with the resulting surface structure representing a compromise between bulk strain release and minimization of the surface free energy. This is reflected in the restructuring of the annular silver tube, taking several days at high temperature (>600 °C) to condition into a "dynamic steady-state morphology" while the silver particles reach this state in a matter of hours at this temperature.

The most important aspect to establish may, however, be how the increase in surface area resulting from the morphology changes relates to the catalyst performance. The extent of restructuring (Fig. 5) and the increase in conversion (Fig. 2) clearly both correlate with the reaction temperature. We have attempted to obtain a surface area increase estimate from Kr physisorption experiments but were so far not successful. This is due to the overall low specific surface area and most other authors also report surface structural changes mainly in terms of SEM morphology. The initial selectivity increase observed supports the notion that the oxygen dissolution in combination with Ag refacetting yield O_γ sites that facilitate the selective methanol to formaldehyde pathway. The slight decrease in formaldehyde selectivity with continued restructuring and conversion increase could reflect a slightly different competition between different pathways as the conversion is increased through the addition of more sites; i.e., enabling more O_α on the surface without the population of O_γ accordingly enhanced.

3.5. Kinetic and mechanistic considerations

One of the objectives of this work has been to extract kinetic parameters for methanol to formaldehyde reaction over silver. Our experiments discussed above prove that the annular reactor concept enables investigations at industrially relevant temperatures and space velocity with low conversions of both methanol and oxygen and very high selectivity to formaldehyde. It is unfortunately not possible to directly extract kinetic parameters from the series presented so far due to different degree of restructuring for the four different furnace setpoints. In order to overcome

the abovementioned challenges, longer 8-day runs at furnace setpoint 600 °C (reference conditions) were performed to pre-condition the catalyst to a higher extent, before performing a stepwise cooling until 500 °C to obtain temperature dependent data. It was then assumed that the restructuring or conditioning effects would be minor within this temperature variation, due to its overall progress towards an (assumed) constant activity and "dynamic steady-state morphology ", relatively short time span of the temperature ramp (12 h) and a gradually slower restructuring upon decreasing the temperature.

The results, plotted against the measured duct temperature, are displayed in Fig. 6a. It may be noted that the formaldehyde selectivity remains high (>97%) for decreasing conversions of methanol and oxygen from 20 to 9% and 25 to 14%, respectively. There is a corresponding increase in the CO_2 selectivity, from 2.1 to 2.5%, upon lowering the temperature. As before, the only carbon products detected were CH_2O and CO_2. An apparent activation energy can be extracted based on methanol conversion using the integral reactor approach as shown in Fig. 6b. First order dependency in methanol is assumed [26], and there is a clear non-linearity below 500 °C that also shows in the conversion plot and will be further commented below. A value of 41 kJ/mol is obtained based on the three highest furnace temperature setpoints. The beneficial characteristics of the annular configuration in avoiding mass transfer limitations at differential conditions play a significant part in achieving the presented activation energy. Preliminary studies, both experimental and theoretical, support that the analyses are under a fully chemical regime.

Since kinetic data for this reaction system at industrially relevant conditions are limited in the literature, there are few relevant estimates of activation energy. Andreasen et al. [26,31] developed a microkinetic model for methanol oxidation with simulated apparent activation enthalpies, however, with a reactant composition corresponding to the average between inlet and outlet of an industrial reactor (without additional water in the feed). Temperature dependent variations in apparent activation enthalpies were obtained due to changes in coverage and thereby the energy barriers, hence emphasizing the difficulty in comparing results obtained at different reaction conditions.

What is clear in Fig. 6, is the conversion plateau between about 500–525 °C, corresponding to 540–560 °C furnace setpoint. The experimental run at 540 °C at constant temperature setpoint also deviated from the higher furnace setpoints (Fig. 2) and this was consistent over several experiments. Comparable behaviors were described by Nagy et al. [19] and Waterhouse et al. [13] with respect to fresh, unconditioned silver particle catalysts. A plateau of low conversion was reported in the range 425–575 °C. Our results from 540 °C setpoint display, in contrast to the higher temperatures, almost constant measured catalyst temperature (~510 °C) and conversion of both methanol and oxygen during time on stream and the selectivity to formaldehyde and H_2/CO_2 ratio never passing through a maximum (Fig. 2). The behavior becomes even more evident from the Arrhenius plot (Fig. 6b), and therefore only the three highest temperatures were included to the apparent activation energy estimate. It seems that different mechanisms are pertaining at the high and low ends of the temperature range, divided at ~500 °C reaction temperature. Nagy et al. [19] also proposed the presence of several different mechanisms due to variation in obtained activation energy values, which were small (2–7 kJ/mol), i.e. even possible diffusion effects. Literature furthermore indicates a third region below 465 °C, corresponding to reactions of surface bonded O_α species formed directly from the gas phase and dominated by high CO_2 production [3–6,18]. Nevertheless, high CH_2O selectivity is present for all the temperatures investigated here, and the high selectivity could imply the presence of the selective O_γ species resulting from dissolution of oxygen (O_β). Finally, both the abovementioned studies found that, after running fresh silver catalyst through several cooling/heating cycles, the high temperature treatment eventually irreversibly modified the catalyst to achieve stable conversion at a level higher than obtained in the initial cycles. The conversion plateau with changing temperature was no longer visible, underlining again the close

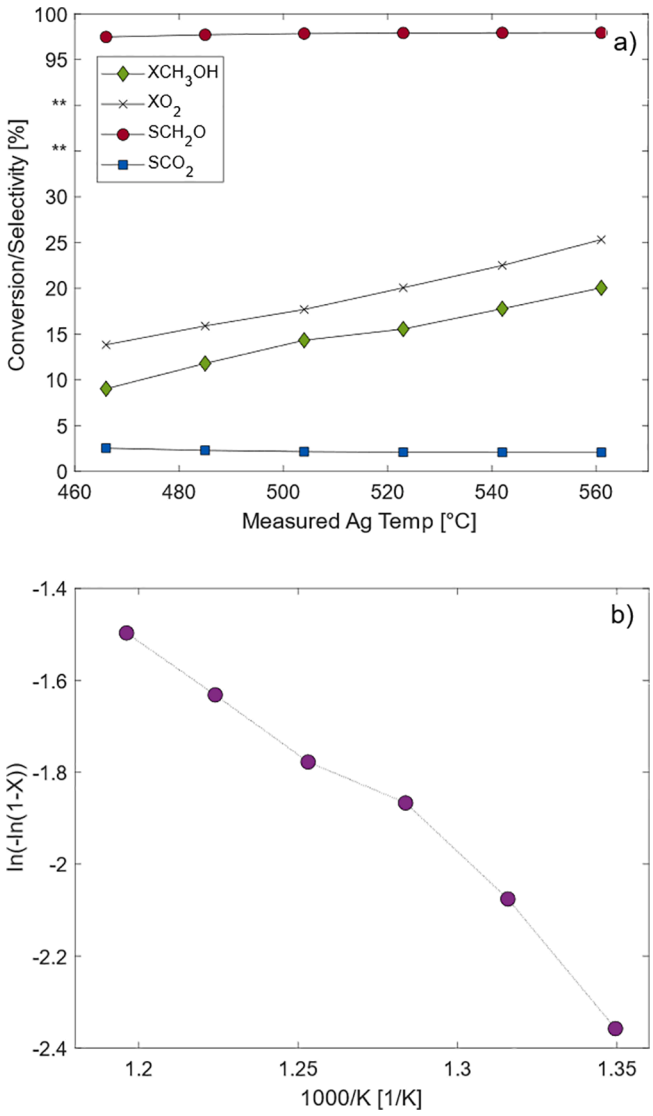

Fig. 6. a) Conversion (CH_3OH and O_2) and product selectivities (CH_2O, CO_2, H_2 and H_2O) as a function of measured Ag duct temperature obtained after MTF reaction for 8 days at 600 °C furnace setpoint temperature. b) Integral reactor Arrhenius plot for the CH_3OH conversion. Reaction conditions: furnace setpoint 500–600 °C, molar feed composition $CH_3OH/H_2O/O_2/N_2$ = 8/11/3/78, total flow rate 250 Nml/min, Ag catalyst tube length 20 mm.

relationship between oxygen dissolution, restructuring, temperature, and activity.

In the case of furnace setpoint 540 °C and without temperature cycling, the moderate restructuring of the silver morphology during time on stream (Fig. 5c) appears insufficient with respect to changing the intrinsic activity. Assuming that the activity increase at higher temperature reflects addition of O_γ sites in the silver surface, oxygen diffusion to form and transport sub-surface oxygen (O_β) becomes essential. Such diffusion in silver may proceed through both grain boundary and interstitial diffusion mechanisms at temperatures below ~625 °C and then vacancy bulk diffusion is enabled above this temperature [5,53,54]. As the reaction temperature is relatively low (<511 °C) for 540–500 °C furnace setpoint, the former mechanisms should dominate. Inhibited or slow oxygen diffusion and thereby limited formation of active oxygen species may thus be part of the explanation to the sustained low conversion in Fig. 2a and b for 540 °C. The corresponding SEM micrographs reveal some pinhole formation, which implies that some oxygen diffusion in silver is taking place, but no "spitting" (Fig. 5c).

In general, the mobility of both (dissolved) oxygen and silver increases with temperature, as can be seen from the increased amount of restructuring, pinholes and spitting in Fig. 5, but so does activity. With higher diffusivity, there is reason to believe that the concentration of O_β is enhanced and availability of O_γ sites increased. Thus, the importance of oxygen and silver interactions in obtaining high activity are once more implied, and one may conclude that oxygen, in some form, is involved in the rate determining phenomena for the overall process. The activation energy for silver oxygen diffusion in the temperature range of 600–950 °C was estimated as 46–48.5 kJ/mole by Bergwerff et al. [59], based on diffusion coefficient measurements from several authors [54,60–65]. Although our apparent activation energy estimate (41 kJ/mol) may include mechanistic aspects beyond oxygen diffusion the compiled evidence could indicate that the rate of oxygen diffusion through silver affects the rate of the overall process.

The reported data suggest that with respect to partial oxidation of methanol to formaldehyde, annular reactors can help bridge lab scale investigations with industrial operation. By enabling kinetic investigations at high space velocity and high reaction temperature, more reliable data for kinetic models are obtained. This includes isolating the role of the silver surface chemistry from that of gas phase contributions and new insight to the primary product formation, as demonstrated by the present study. There is a clear opportunity for obtaining better understanding of sub-reaction systems, secondary reactions, and the role of H_2O, and such investigations will be targeted. Albeit not having reached this stage in the current work, there is also potential to disentangle further the effects of oxygen dissolution in the silver on the catalysis and possibly combine with spectroscopic characterization. The mechanistic and kinetic insight can be integrated into (industrial) reactor models that also incorporate mass transfer and gas phase contributions. Eventually, the results can point to improvements in reactor or catalyst design that can further enhance the CH_2O yield.

4. Conclusions

A structured reactor with annular configuration was successfully applied for studying the silver catalyzed methanol oxidation to formaldehyde. By eliminating gas phase reactions, high formaldehyde selectivity (93–97%) was obtained at low methanol and oxygen conversion under practically isothermal reaction conditions. The only carbon containing products detected were CH_2O and CO_2, and both may be claimed as primary products along with H_2. The lack of CO proves that its formation is a result of homogenous decomposition of CH_2O and that it should not considered as the main precursor to CO_2 as assumed in several proposed reaction mechanisms. The analysis of H_2/CO_2 ratio as a function of temperature provides an estimate of the contributions from dehydrogenation and partial oxidation of methanol. The presence of a dehydrogenation pathway to CH_2O seems apparent, except at the highest partial pressure of oxygen. Extracting kinetic parameters proved challenging due to close relationship between activity, oxygen dissolution, and silver restructuring and morphology, and its dependence on temperature. Nevertheless, conversion increased with increasing oxygen concentration, indicating 1st order dependency. Conditioning by reaction at high temperature followed by a temperature ramp down was made in order to minimize the impact of a gradually changing Ag catalyst. The resulting Arrhenius plot indicated two distinct regions of activity and the apparent activation energy was estimated as ~ 41 kJ/mol for the high temperature region. This value is close to the activation energy for oxygen diffusion in silver at high temperature. The investigation demonstrates benefits of using an annular reactor configuration in bridging lab scale investigations with industrial operation and enabling investigations at low conversion that have not been achievable in conventional lab scale reactors this far.

Declaration of Competing Interest

The authors declare that they have no known competing financial interests or personal relationships that could have appeared to influence the work reported in this paper.

Acknowledgement

The authors would like to thank master students Susanne K. Stokkevåg and Nikolas Beck, NTNU, for performing SEM characterization and initial annular reactor tests, respectively. This publication forms a part of the iCSI (industrial Catalysis Science and Innovation) Centre for Researched-based Innovation, receiving financial support from the Research Council of Norway under contract no. 237922. We gratefully acknowledge discussions with Thomas By at K.A. Rasmussen, and with Alessandra Beretta, Politecnico di Milano, and Enrique Iglesia, UC Berkeley, both scientific advisors to iCSI.

References

[1] G.J. Millar, M. Collins, Industrial & Engineering Chemistry Research 56 (33) (2017) 9247–9265, https://doi.org/10.1021/acs.iecr.7b02388.
[2] A. W. Franz, H. Kronemayer, D. Pfeiffer, R. D. Pilz, G. Reuss, W. Disteldorf, A. O. Gamer and A. Hilt. Ullmann's Encyclopedia of Industrial Chemistry (2016).https://doi.org/10.1002/14356007.a11_619.pub2.
[3] L. Lefferts, J. Van Ommen, J. Ross, Applied catalysis 23 (2) (1986).
[4] G.I.N. Waterhouse, G.A. Bowmaker, J.B. Metson, Applied Catalysis A: General 265 (1) (2004) 85–101, https://doi.org/10.1016/j.apcata.2004.01.016.
[5] A. Nagy, G. Mestl, Applied Catalysis A: General 188 (1–2) (1999) 337–353, https://doi.org/10.1016/S0926-860X(99)00246-X.
[6] A. Nagy, G. Mestl, T. Rühle, G. Weinberg, R. Schlögl, Journal of Catalysis 179 (2) (1998) 548–559, https://doi.org/10.1006/jcat.1998.2240.
[7] A.J. Nagy, G. Mestl, D. Herein, G. Weinberg, E. Kitzelmann, R. Schlögl, Journal of Catalysis 182 (2) (1999) 417–429, https://doi.org/10.1006/jcat.1998.2388.
[8] H. Schubert, U. Tegtmeyer, R. Schlögl, Catalysis letters 28 (2–4) (1994) 383–395, https://doi.org/10.1007/BF00806069.
[9] M. Qian, M. Liauw and G. Emig. 238 (2) (2003) 211–222, https://doi.org/10.1016/S0926-860X(02)00340-X.
[10] F. Johnson, P. Larose, Journal of the American Chemical Society 46 (6) (1924) 1377–1389, https://doi.org/10.1021/ja01671a006.
[11] E.W.R. Steacie, F. Johnson, Proceedings of the Royal Society of London, Series A, Containing Papers of a Mathematical and Physical Character 112 (762) (1926) 542–558, https://doi.org/10.1098/rspa.1926.0128.
[12] S. Lervold, K. Arnesen, N. Beck, R. Lødeng, J. Yang, K. Bingen, J. Skjelstad, H. J. Venvik, Topics in Catalysis 62 (7) (2019).
[13] G.I.N. Waterhouse, G.A. Bowmaker, J.B. Metson, Applied Catalysis A: General 266 (2) (2004) 257–273, https://doi.org/10.1016/j.apcata.2004.02.015.
[14] G.J. Millar, M.L. Nelson, P.J. Uwins, Journal of Catalysis 169 (1) (1997).
[15] X. Bao, J. Barth, G. Lehmpfuhl, R. Schuster, Y. Uchida, R. Schlögl, G. Ertl, Surface science 284 (1–2) (1993).
[16] X. Bao, M. Muhler, B. Pettinger, Y. Uchida, G. Lehmpfuhl, R. Schlögl, G. Ertl, Catalysis letters 32 (1–2) (1995) 171–183, https://doi.org/10.1007/BF00806112.
[17] C. Rehren, M. Muhler, X. Bao, R. Schlögl, G. Ertl, Zeitschrift für Physikalische Chemie 174 (1) (1991) 11–52, https://doi.org/10.1524/zpch.1991.174.Part_1.011.
[18] G.I.N. Waterhouse, G.A. Bowmaker, J.B. Metson, Applied surface science 214 (1–4) (2003) 36–51, https://doi.org/10.1016/S0169-4332(03)00350-7.
[19] G.J. Millar, J.B. Metson, G.A. Bowmaker, R.P. Cooney, Journal of the Chemical Society, Faraday Transactions 91 (22) (1995) 4149–4159, https://doi.org/10.1039/FT9959104149.
[20] L. Lefferts, J. Van Ommen and J. Ross. Applied catalysis 34 (1987) 329-339. https://doi.org/10.1016/S0166-9834(00)82466-5.
[21] L. Lefferts, J. Van Ommen, J. Ross, Applied catalysis 31 (2) (1987) 291–308, https://doi.org/10.1016/S0166-9834(00)80698-3.
[22] L. Lefferts, J.G. Van Ommen, J.R. Ross, Journal of the Chemical Society, Faraday Transactions 1: Physical Chemistry in Condensed Phases 83 (10) (1987) 3161–3165, https://doi.org/10.1039/F19878303161.
[23] S. Bhattacharyya, N. Nag, N. Ganguly, Journal of Catalysis 23 (2) (1971) 158–167, https://doi.org/10.1016/0021-9517(71)90037-6.
[24] D.A. Robb, P. Harriott, Journal of Catalysis 35 (2) (1974) 176–183, https://doi.org/10.1016/0021-9517(74)90194-8.
[25] I.E. Wachs, R. Madix and 76 (2) (1978) 531–558, https://doi.org/10.1016/0039-6028(78)90113-9.
[26] A. Andreasen, H. Lynggaard, C. Stegelmann, P. Stoltze, Surface Science 544 (1) (2003).
[27] E. Cao, A. Gavriilidis, Catalysis today 110 (1–2) (2005) 154–163, https://doi.org/10.1016/j.cattod.2005.09.005.
[28] C.B. Wang, G. Deo, I.E. Wachs, The Journal of Physical Chemistry B 103 (27) (1999) 5645–5656, https://doi.org/10.1021/jp984363l.

[29] X. Bao, J. Deng, Journal of Catalysis 99 (2) (1986) 391–399, https://doi.org/10.1016/0021-9517(86)90364-7.
[30] W. Sim, P. Gardner, D. King, The Journal of Physical Chemistry 99 (43) (1995) 16002–16010, https://doi.org/10.1021/j100043a046.
[31] A. Andreasen, H. Lynggaard, C. Stegelmann, P. Stoltze, Applied Catalysis A: General 289 (2) (2005) 267–273, https://doi.org/10.1016/j.apcata.2005.05.004.
[32] A.C. van Veen, O. Hinrichsen, M. Muhler, Journal of Catalysis 210 (1) (2002) 53–66, https://doi.org/10.1006/jcat.2002.3682.
[33] X. Bao, M. Muhler, B. Pettinger, R. Schlögl, G. Ertl, Catalysis letters 22 (3) (1993) 215–225, https://doi.org/10.1007/BF00810368.
[34] X. Bao, M. Muhler, T. Schedel-Niedrig, R. Schlögl, Physical Review B 54 (3) (1996) 2249, https://doi.org/10.1103/PhysRevB.54.2249.
[35] L. Lefferts, J.G. Van Ommen, J.R. Ross, Journal of the Chemical Society, Faraday Transactions 1: Physical Chemistry in Condensed Phases 84 (5) (1988) 1491–1499, https://doi.org/10.1039/F19888401491.
[36] Q. Sun, B. Shen, K. Fan, J. Deng, Chemical Physics Letters 322 (1–2) (2000) 1–8, https://doi.org/10.1016/S0009-2614(00)00396-1.
[37] Q. Sun, Y. Wang, K. Fan, J. Deng, Surface science 459 (1–2) (2000) 213–222, https://doi.org/10.1016/S0039-6028(00)00484-2.
[38] R. Beuhler, R. Rao, J. Hrbek, M. White, The Journal of Physical Chemistry B 105 (25) (2001) 5950–5956, https://doi.org/10.1021/jp010134e.
[39] H. Schubert, U. Tegtmeyer, D. Herein, X. Bao, M. Muhler and R. Schlögl. 33 (3–4) (1995) 305–319, https://doi.org/10.1007/BF00814233.
[40] A.D. Schlunke, Mechanism and Modelling of the Partial Oxidation of Methanol over Silver, The University of Sydney, In School of Chemical and Biomolecular Engineering, 2007.
[41] J.G. McCarty, Catalysis Today 26 (3–4) (1995) 283–293, https://doi.org/10.1016/0920-5861(95)00150-7.
[42] W. Ibashi, G. Groppi, P. Forzatti, Catalysis today 83 (1–4) (2003) 115–129, https://doi.org/10.1016/S0920-5861(03)00221-9.
[43] A. Beretta, P. Baiardi, D. Prina, P. Forzatti, Chemical Engineering Science 54 (6) (1999) 765–773, https://doi.org/10.1016/S0009-2509(98)00261-9773.
[44] A. Beretta, E. Ranzi, P. Forzatti, Chemical Engineering Science 56 (3) (2001) 779–787, https://doi.org/10.1016/S0009-2509(00)00289-X.
[45] H. Redlingshöfer, O. Kröcher, W. Böck, K. Huthmacher, G. Emig, Industrial & engineering chemistry research 41 (6) (2002) 1445–1453, https://doi.org/10.1021/ie0106074.
[46] K. Venkataraman, E. Wanat, L. Schmidt, AIChE Journal 49(5) (2003).
[47] I. Aartun, T. Gjervan, H. Venvik, O. Görke, P. Pfeifer, M. Fathi, A. Holmen, K. Schubert, Chemical Engineering Journal 101 (1–3) (2004) 93–99, https://doi.org/10.1016/j.cej.2004.01.006.
[48] A. Beretta, G. Groppi, L. Majocchi, P. Forzatti, Applied Catalysis A: General 187 (1) (1999) 49–60, https://doi.org/10.1016/S0926-860X(99)00182-9.
[49] T. Bruno, A. Beretta, G. Groppi, M. Roderi, P. Forzatti, Catalysis today 99 (1–2) (2005) 89–98, https://doi.org/10.1016/j.cattod.2004.09.027.
[50] I. Tavazzi, A. Beretta, G. Groppi, P. Forzatti, An investigation of methane partial oxidation kinetics over Rh-supported catalysts, Studies in surface science and catalysis, Elsevier (2004) 163–168, https://doi.org/10.1016/S0167-2991(04)80045-4.
[51] A. Donazzi, A. Beretta, G. Groppi, P. Forzatti, Journal of Catalysis 255 (2) (2008) 241–258, https://doi.org/10.1016/j.jcat.2008.02.009.
[52] A. Donazzi, A. Beretta, G. Groppi, P. Forzatti, Journal of Catalysis 255 (2) (2008) 259–268, https://doi.org/10.1016/j.jcat.2008.02.010.
[53] R. Outlaw, D. Wu, M. Davidson, G.B. Hoflund, Journal of Vacuum Science Technology A: Vacuum, Surfaces, Films 10 (4) (1992) 1497–1502, https://doi.org/10.1116/1.578273.
[54] R. Outlaw, S. Sankaran, G. Hoflund, M. Davidson, Journal of Materials Research 3 (6) (1988) 1378–1384, https://doi.org/10.1557/JMR.1988.13781378-1384.
[55] M.A. Barteu, R.J. Madix, The Chemical Physics of Solid Surfaces and Heterogeneous Catalysis 4 95–142 (1982). ISBN: 044441987X/0444419713.
[56] G.J. Millar, M.L. Nelson, P.J. Uwins, Journal of the Chemical Society, Faraday Transactions 94 (14) (1998).
[57] P.J. Uwins, G.J. Millar, M.L. Nelson, Microscopy research technique 36 (5) (1997) 382–389.
[58] X. Bao, G. Lehmpfuhl, G. Weinberg, R. Schlögl, G. Ertl, Journal of the Chemical Society 88 (6) (1992) 865–872, https://doi.org/10.1039/FT9928800865.
[59] J. Bergwerff and A. van Dillen. Universiteit Utrecht. http://www.projects.science.uu.nl/anorg/PDF/Bergwerff_silver%20literature.pdf.
[60] V. Gryaznov, S. Gulyanov, S. Kanizius, Russian Journal of Physical Chemistry 47 (10) (1973) 1517–1518.
[61] H. Rickert, R. Steiner, Zeitschrift für Physikalische Chemie 49 (35) (1966).
[62] J. Bazan, Electrochimica Acta 13 (8) (1968).
[63] W. Eichenauer and G. Miller. NASA Technical Memorandum TM-77938 (1985). NASA-TM-77938 19860012184.
[64] J.H. Park, Materials letters 9 (9) (1990).
[65] T. Ramanarayanan, R. Rapp, Metallurgical transactions 3 (12) (1972).